Computing Sheet Rolling Instabilities with a Shell Finite Element Model

A. Cometa(✉), H. J. M. Geijselaers, J. Havinga, and A. H. van den Boogaard

Faculty of Engineering Technology, Chair of Nonlinear Solid Mechanics, University of Twente, 7500 AE Enschede, The Netherlands
a.cometa@utwente.nl

Abstract. In this paper a novel model for 3D finite element sheet metal rolling calculations is presented. A global model which represents the behavior and stress state of the strip outside the roll bite is coupled to a local model which represents in detail the mechanics of deformation within the roll bite. Shell finite elements are used for the global model of the rolled sheet, while 2D plane strain elements are used for the local model of the strip and the roll. The coupling is made via an equivalent roll bite model, incorporated into the shell model to represent the physics of the roll bite. The rolling velocity, the zero out-of-plane position and the thickness strain are enforced at the roll line via a set of constraint equations. The amount of prescribed thickness reduction is determined based on the local tensions and friction coefficient. A metamodel which provides the relation between these conditions and the local thinning is obtained from 2D off-line rolling calculations. The proposed model can be used instead of a full 3D rolling model, as it is computationally less expensive, especially for thin strip rolling simulations. It is shown how the developed model can be applied to analyze instability phenomena in cold rolling processes, specifically strip buckling due to disruptions in the process conditions.

Keywords: Thin strip rolling · Steel sheets · Flatness defects

1 Introduction

3D finite element models of strip rolling are used to simulate the deformation and stress distribution in a rolling process. With these models sensitivity analyses can be performed to evaluate the effect of changes in the process settings on the rolling behavior. Sensitivity analyses can help to identify critical parameters that affect the stability of the rolling process and the quality of the final products. For example, 3D FEM models are a very useful tool to investigate the occurrence of flatness defects in rolling processes [1,7,8,13]. Flatness defects in sheet rolling are caused by inhomogeneous deformations in the roll bite across the width of the sheet. These can be caused by a number of factors, including variations in the roll gap (thermo-elastic roll deformation) and variations in the material properties of the sheet. Inhomogeneous deformations can result in

K. Mocellin et al. (Eds.): ICTP 2023, LNME, pp. 541–552, 2024.
https://doi.org/10.1007/978-3-031-40920-2_56

non-uniform stress distributions within the sheet, with local compressive stresses which can induce buckling [5]. These phenomena can lead to a variety of defects in the rolled sheet, such as waviness (e.g. center buckles and wavy edges [7,10]), wrinkles [1], or pinching [3,4]. Pinching in sheet metal rolling refers to the occurrence of defects, that appear as repetitive ripples, waviness, surface marks and local ruptures. Pinching can also cause damage to the rolling mill itself, leading to downtime and increased maintenance costs. It was shown experimentally that pinching defects can be induced by non-uniform frictional conditions between the sheet and the rolls, due to disruptions in the lubrication during rolling [4]. In an industrial rolling mill, there are several potential causes of disruptions in the lubrication, that result in a change of the frictional conditions between the strip and the roll. These can include inadequate lubricant application or distribution, changes in the viscosity or composition of the lubricant [3], or contamination of the lubricant with foreign particles [14]. It was observed that due to disturbances in the lubrication conditions buckles may appear in front of the roll bite. These buckles get trapped between the rolls, resulting in folds in the metal, which will finally appear as repetitive ripples. To capture the mechanism of formation of flatness defects, both a detailed local model of the roll bite and a global model of the strip are needed. Moreover, the conditions outside the roll bite (stress distribution and onset of instabilities) have a significant interaction with the conditions within the roll bite. Therefore, it is crucial to ensure the coupling between the conditions inside and outside the roll bite [1,2]. However, it is computationally very expensive to perform 3D rolling simulations based on conventional FEM models. The high computational cost of 3D FEM rolling models is due to the size of the simulation domain, which must cover the full thickness and width and enough length of the rolled sheet, and to the resolution of the mesh, which needs to be high in the roll bite, where high gradients of deformation occur. This leads to very large models, especially for thin strip rolling [6,12].

To reduce the computational cost of 3D rolling simulations a novel strategy is presented in this paper. The sheet is modeled using shell finite elements. In this shell model the mechanical interaction between the strip and the work rolls is reproduced via an equivalent roll bite model. A set of constraints is applied to the shell finite elements crossing the roll line, to enforce the rolling velocity, the zero out-of-plane position and the thickness reduction. A metamodel is used to couple the prescribed thickness reduction to the local tensions and friction coefficient. By using the equivalent roll bite model, sheet rolling calculations can be performed more efficiently compared to full 3D FEM simulations. The proposed method is applied to model instability phenomena which arise from disruptions in the lubrication conditions during cold rolling. It is shown that, by using the equivalent roll bite model for shell rolling calculations, it is possible to simulate flatness defects in sheet metal rolling. Various scenarios are analyzed to study the behavior of the rolled sheet when different types of disruptions in the lubrication conditions are applied.

2 Equivalent Roll Bite Model

A graphical overview of the equivalent roll bite model is given in Fig. 1. A global shell finite element model of the strip is considered in the x–y plane, being x the rolling direction, as shown in Fig. 1a. Three-dimensional 3-node Discrete Kirchhoff Triangles are used for the finite element discretization. In the global model, the strip is subjected to the entry and exit tension forces, T_{in} and T_{out}. A roll line is defined parallel to the y-axis. A numerical algorithm is used to enforce a set of constraint conditions to the shell elements crossing the roll line. These constraints allow to reproduce in the global model the mechanics of the roll bite, as described in Sect. 2.1. The strip is seen as a collection of adjacent slices. Each slice is represented as a plane-strain problem, using a local 2D ALE model, as shown in Fig. 1b. Input parameters for the 2D model are: the geometrical parameters (roll radius R, roll center distance D and strip's entry thickness H), the roll and strip material parameters and the local conditions occurring in each slice, that are the specific entry and exit tensions, t_{in} and t_{out}, and the friction coefficient μ. The global and the local models are coupled to ensure a continuous update of the conditions inside and outside the roll bite, as explained in Sect. 2.2.

2.1 Constraint Conditions

The finite element rolling simulation is performed using the incremental analysis, based on the Updated Lagrangian method. The conditions of rolling velocity, zero out-of-plane position and thickness strain are enforced to the elements crossing the roll line in the current time increment n. The configurations of the shell element at the beginning and at the end of the calculation step n are shown in Fig. 2.

Rolling Velocity. At the beginning of the current step, for any element passing over the roll line, the intersection points, P_1 and P_2, are first identified. The incremental x-displacements of those points can be expressed as a function of the incremental nodal x-displacements $\{\mathbf{d}_x\}$ via the shape functions matrix $[\mathbf{N}]$. At the intersection points the rolling velocity d_{R} is prescribed. The constraint equation to be satisfied is:

$$\mathbf{c}_{\text{R}}(\{\mathbf{d}_x\}) = [\mathbf{N}]\{\mathbf{d}_x\} - d_{\text{R}}\{\mathbf{1}\} = \mathbf{0} \tag{1}$$

The rolling velocity constraint equation corresponds to two linearly independent scalar equations, one for each intersection point.

Zero Out-of-Plane Position. The zero out-of-plane position is enforced at the roll line, which allows to restrain the strip's z-displacement due to the presence of the rolls. The current z-position of the two intersection points, represented by the vector $\{\mathbf{z}_{\text{P}}\}$, can be obtained by interpolating the current nodal z-coordinates via the shape functions. The constraint equation to be satisfied is:

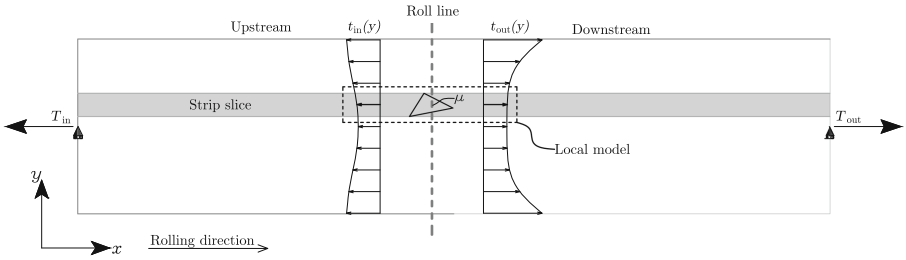

(a) Global shell finite element model of the strip

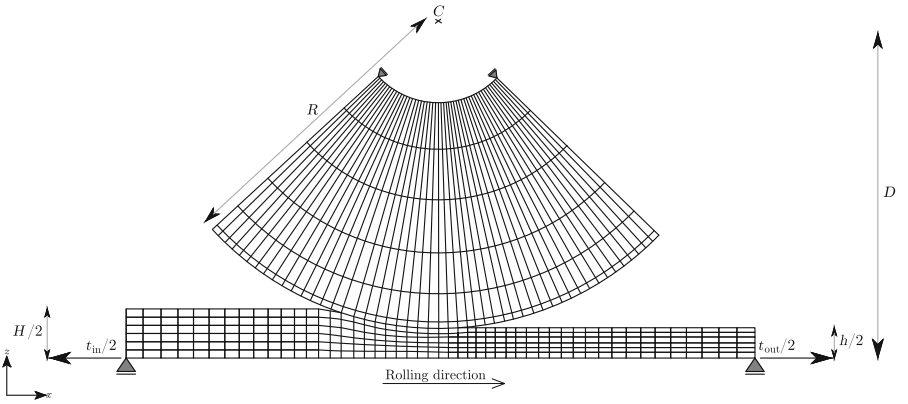

(b) 2D local model of the roll bite

Fig. 1. Overview of the equivalent roll bite model.

$$\mathbf{c}_{\mathrm{z}}(\{\mathbf{d}\}) = \{\mathbf{z}_{\mathrm{P}}\}(\{\mathbf{d}\}) = \mathbf{0} \tag{2}$$

where $\{\mathbf{d}\}$ is the set of nodal incremental displacements in x, y, and z directions.

Thickness Strain. The thickness strain constraint allows to enforce a certain thickness strain ε_{zz} by changing the element area. The area of the shell element crossing the roll line is increased by an amount which is proportional to the fraction of the element area that is rolled in the current step, A^n_{rol}, and to the area strain, $\varepsilon^n_{\mathrm{A}}$. The latter one can be defined as function of the thickness strain. Here, for simplicity, the area strain is approximated as:

$$\varepsilon^n_{\mathrm{A}} \approx -\varepsilon^n_{zz} \tag{3}$$

The constraint equation to be satisfied is:

$$c_{\mathrm{A}}(\{\mathbf{d_{xy}}\}) = A^{n+1}(\{\mathbf{d_{xy}}\}) - [A^n + A^n_{\mathrm{rol}} \cdot \varepsilon^n_{\mathrm{A}}] = 0 \tag{4}$$

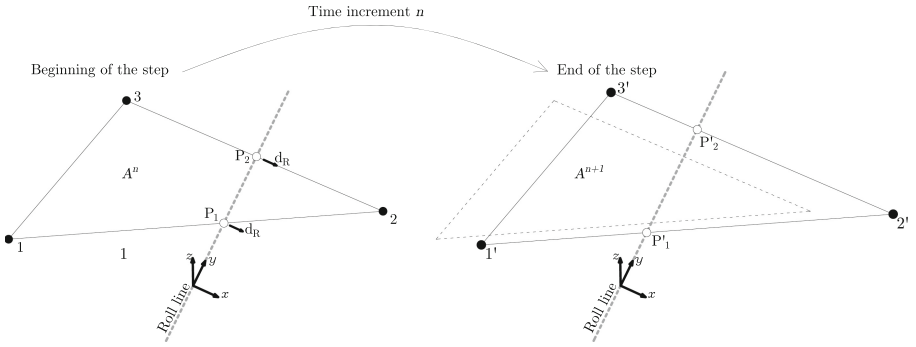

Fig. 2. Shell element crossing the roll line during the current time increment n.

where $\{\mathbf{d_{xy}}\}$ is the set of incremental nodal displacements in x and y directions. The prescribed change of the element area results in both a longitudinal strain (strain in the rolling direction) and a transversal strain. This allows to account for material later flow during rolling.

To enforce the constraints given by Eqs. (1), (2) and (4), the penalty method is used. For any element currently crossing the roll line, this results in a modified stiffness matrix and force vector. In this way, a modified global system of equations is solved at each time increment.

2.2 Metamodel

The plastic deformations occurring in the roll bite affect the in-plane stress state outside the roll bite and vice-versa. Therefore, to achieve accurate results, the reciprocal influence between the global and the local mechanical behavior of the rolled sheet must be accounted for. This is of particular importance when modeling the effect of disruptions on the rolling behavior. When a local disturbance occurs during the process (e.g. variations in the lubrication conditions, in the profile of the strip or the roll, or in the material properties), the local deformation of the strip being rolled changes. This results in a stress re-distribution outside the roll bite, which will in turn affect the in-bite deformations. Therefore, in the proposed model, the thickness strain prescribed at the roll line is obtained as a function of the local tensions and friction coefficient. The coupling between in-bite and out-of-bite conditions is enabled via a metamodel, which is built from off-line rolling calculations, using a refined 2D ALE model of the roll bite, as shown in Fig. 1b. A set of rolling simulations is performed for a specific rolling process (stand geometry, strip entry thickness and material properties), considering a range of different entry and exit tensions and different friction coefficients. The results of these simulations are used to define the thickness strain as function of the local tensions and friction coefficient.

3 Application to Thin Strip Rolling

The developed model is used to perform thin strip rolling simulations. The aim is to analyze the behavior of the strip during the rolling process, including the occurrence of instabilities due to disruptions in the lubrication conditions.

Model Input. A sheet of low carbon packaging steel is rolled, undergoing a thickness reduction of 22.35% (at the strip center line). The input parameters for the model are summarized in Table 1. An isotropic elasto–plastic material model with Swift hardening is used for the strip. The yield stress is expressed as $\sigma_y(\bar{\varepsilon}^{\mathrm{p}}) = \sigma_{y0} + C \cdot (\bar{\varepsilon}^{\mathrm{p}} + \varepsilon_0)^n$, where $\bar{\varepsilon}^{\mathrm{p}}$ is the equivalent plastic strain, σ_{y0} is the offset yield stress, ε_0 is the offset yield strain, C is the hardening modulus and n is the Swift power law variable. For the considered rolling case two metamodels are constructed which give the thickness reduction as a function of the entry and exit local tensions, for two levels of friction: one for $\mu_{\mathrm{low}} = 0.025$ and one for $\mu_{\mathrm{high}} = 0.1$. The lower friction coefficient, which is within a typical range for a well lubricated cold rolling process [11], leads to a value of the total roll force approximately equal to 550 kN. On the other hand, the higher friction coefficient is assumed for a non-lubricated rolling process.

Table 1. Input parameters of the shell rolling model.

Process parameters		
Strip's width	W	180 mm
Strip's length	L	1440 mm
Strip's entry thickness	H	0.255 mm
Roll radius	R	198.5 mm
Roll center distance	D	198.527 mm
Entry tension force	T_{in}	4.5 kN
Exit tension force	T_{out}	5.5 kN
Material parameters		
Elasticity modulus	E	200 GPa
Poisson's ratio	ν	0.3
Offset yield stress	σ_y	397 MPa
Offset yield strain	ε_0	0.0588
Hardening modulus	C	630 MPa
Swift power law variable	n	0.1632

First the rolling simulation is performed considering uniform good lubrication conditions ($\mu_{\mathrm{low}} = 0.025$) over the strip's width. The simulation is continued until steady-state conditions are reached. Thereafter, a disturbance is introduced, by applying $\mu_{\mathrm{high}} = 0.1$, on a portion of the strip width. This is shown in Fig. 3,

where the lubricated and non-lubricated patches are highlighted on top of the shell finite element mesh. Two scenarios are considered, to study the sensitivity of the results to the width of the lubricated/non-lubricated patches. In the second scenario being analyzed, there is a disruption in the lubrication conditions that is the opposite of the first scenario. In the first scenario, the lubricated patch has a width of 60 mm. In the second scenario, the lubricated patch has a width of 120 mm.

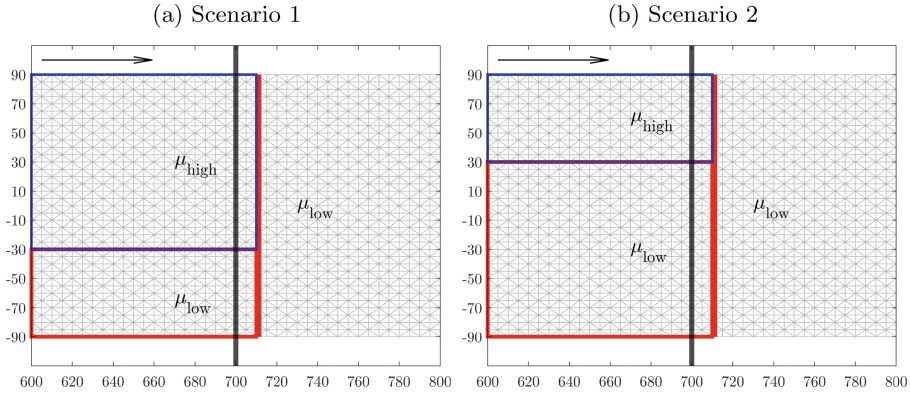

Fig. 3. Application of lubrication disturbance during the rolling simulation.

The first scenario is chosen as a representative example of one of the experimental observations reported in the previous work [4]. Figure 4 shows two consecutive photo frames taken during the pinching experiments from the upstream side of the roll bite. When there is uneven lubrication, with the roll bite becoming mostly dry and local traces of lubricant being present on the strip, the sheet experiences waviness upstream of the roll bite. By simulating the first scenario, it is possible to verify whether the developed model can be used to identify the pinching mechanism observed during the experiments. The second scenario is chosen as a more technologically relevant case, in which insufficient lubrication can locally occur, due to several factors, like nozzle clogging, presence of contaminants or impurities, or changes in the lubricant composition [3] or viscosity.

Simulation Results. Figure 5 shows how the distribution of the longitudinal stress (stress acting in the rolling direction) changes from the steady-state to the state after disruption. In both scenarios, it can be seen that due to the applied disturbance, local compressive stresses develop mainly upstream of the roll line, while local higher tensile stresses occur mainly downstream of the roll line. The most compressive stresses are localized in the lubricated patch, while the higher tensile stresses appear near the line of transition between the lubricated and the non-lubricated patch.

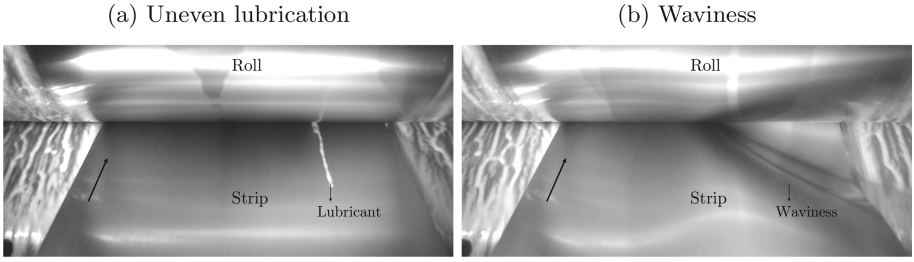

Fig. 4. Experimental observations from a pinching test [4].

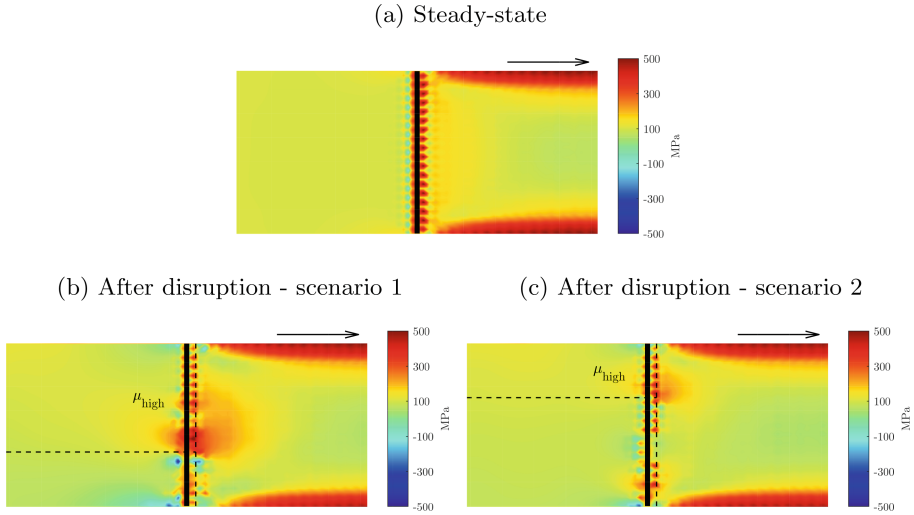

Fig. 5. Longitudinal stress σ_{xx}

The likelihood of buckling in the sheet depends on the most compressive principal stresses. Figure 6 shows the distribution of these stresses upstream of the roll line for both scenarios at the moment before stress relaxation occurs due to the first buckles appearing on the upstream side.

The magnitudes of the compressive principal stresses are higher in the first scenario. If the compressive principal stress in the sheet exceeds a critical value, buckling occurs. The critical buckling stress depends on the geometry (thickness and width) of the sheet, on its material properties, and on the boundary conditions. The out-of-plane displacements induced by the applied disruptions are shown in Fig. 7. It must be noted that there is no steady-state after the disruption is applied, and the results are taken at a specific moment in time shortly after application of the disruption. In both scenarios the strip experiences waviness, not only downstream but also upstream of the roll line. The buckling behavior is shown in Fig. 8. The buckles upstream of the roll line are confined to the part of the strip where the lower friction coefficient is applied.

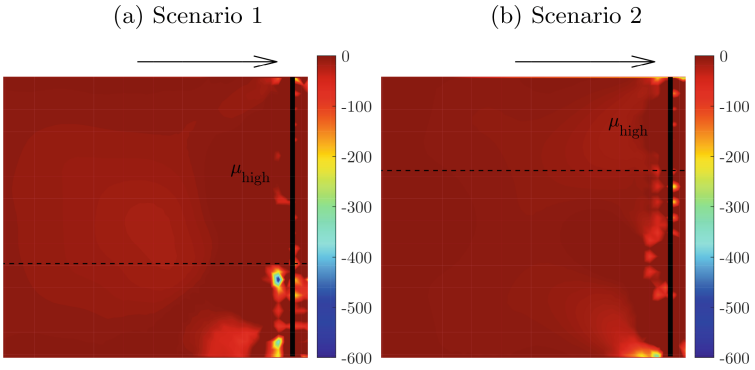

Fig. 6. Compressive principal stress after disruption (before stress relaxation), upstream of the roll line.

However, in the occurrence of the waviness upstream of the roll line, a difference exists between the two scenarios, that has to do with the different level of compressive principal stresses, which is lower in the second scenario than in the first one. In the second scenario, as the rolling process continues, these stresses accumulate and eventually result in buckling, which occurs later than in the first scenario. This difference can be better expressed in terms of length of the sheet being rolled from the moment of disruption to the appearance of buckles on the upstream side. This length is equal to 2.2 mm in the first scenario and to 3.2 mm in the second scenario.

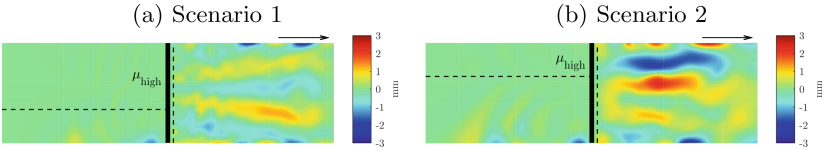

Fig. 7. Out-of-plane displacements induced by the disruption.

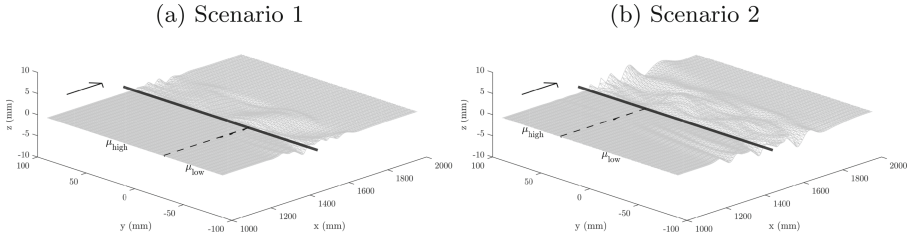

Fig. 8. Buckling behavior of the strip after disruption.

The appearance of tears has also been reported in previous experiments [4]. These are caused by excessive tensile principal stresses in the rolled sheet. These stresses are shown in Fig. 9 for the two scenarios. Consistently in the two cases, the highest magnitudes appear close to the line of transition between the lubricated and the non-lubricated patch. In the first scenario, these stresses are higher and approximately aligned with the most compressive stresses upstream of the roll line.

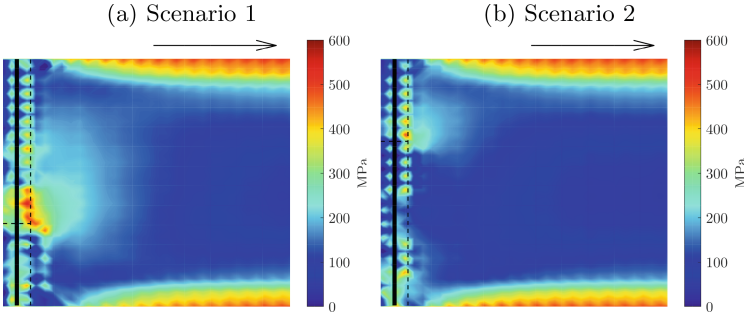

Fig. 9. Tensile principal stress after disruption, downstream of the roll line.

4 Discussions

3D finite element models are an effective tool for simulating the rolling behavior under different conditions. These models can be specifically applied to analyze instabilities in thin strip rolling, which can arise due to various factors. The proposed method for 3D sheet rolling calculations was used to study the effect of uneven lubrication conditions on the stress state and stability of the rolled sheet. The simulation results showed how a local disruption in the frictional conditions affects the rolling process, providing some insights into the complex interplay between lubrication, rolling conditions, and sheet behavior. It was shown that a local variation of the friction coefficient across the strip width causes a stress re-distribution in the rolled sheet. The most significant effects of this disruption are the local lower tensile and even compressive stresses upstream of the roll bite and the local higher tensile stresses downstream of the roll bite. Consistently for the two analyzed cases, the most compressive principal stresses occur locally in the part of the sheet where a lower friction coefficient is applied. If the most compressive principal stress reaches the critical buckling stress, waviness appears in the sheet. Differently from what is commonly described in literature concerning the occurrence of flatness defects [1,9], it was shown that waviness can appear not only downstream of the roll bite, but also upstream. Moreover, unlike other types of flatness defects (e.g. center buckles and wavy edges), the simulated buckles are not always fully aligned with the rolling direction. The compressive principal stresses can take more or less time during the process to build up and

lead to buckles, depending on the type of disruption, as shown in the comparison between the two scenarios. This can be one of the factors influencing the distance between repetitive ripples in pinched strips. The deformed configuration of the buckled strip resembles qualitatively the behavior observed during the pinching experiments, as reported in previous work [4]. Another result of interest that was shown is the local high concentration of tensile principal stress, downstream of the roll line, around the boundary between the lubricated and the non-lubricated patches. The most tensile principal stress is higher than the yield stress of the material in both the two analyzed scenarios. If the tensile principal stress is higher than the ultimate tensile stress of the material, the sheet will experience tears as observed in some pinching experiments. The similarity between simulation results and experimental observations suggests that the proposed model is able to capture the underlying mechanism of pinching or similar types of defects. In this way, the model can contribute to a better understanding of instability phenomena in thin strip rolling. However, it is important to note that the proposed method has a limitation, due to not accounting for the elastic bending of the rolls. This deformation can affect the final shape and thickness of the sheet metal, with a significant effect on its flatness.

5 Conclusions

3D FEM models are a useful tool to simulate and analyze the sheet metal rolling process. These models allow to predict stress and strain distributions in the sheet metal. These predictions can be used to optimize the process parameters and improve the quality of the final products. In this paper a strategy to reduce the computational cost of 3D sheet rolling calculations has been presented. The deformations within the roll bite and the stress distribution outside the roll bite influence each other. This interplay has a critical role in determining the stress and strain fields in the rolled sheet. To account for the mutual influence between in-bite and out-of-bite conditions, an equivalent roll bite model is developed to be connected to a shell model of the sheet. The local deformations within the roll bite are coupled to the local tensions and frictional conditions. The shell model describes the deformation and stress state of the entire sheet. It is shown that a qualitative study of instability phenomena in thin strip rolling can be performed using the proposed model. The rolling behavior which arises from disruptions in the lubrication conditions is analyzed, with a focus on the occurrence of pinching phenomena. Hence, the proposed model has the potential to provide valuable insights into certain complex phenomena which can occur during the rolling process, like those leading to flatness defects.

Acknowledgments. This research was carried out under project number S16039 in the framework of the Partnership Program of the Materials innovation institute M2i and the Technology Foundation TTW, which is part of the Netherlands Organization for Scientific Research.

References

1. Abdelkhalek, S., Montmitonnet, P., Legrand, N., Buessler, P.: Coupled approach for flatness prediction in cold rolling of thin strip. Int. J. Mech. Sci. **53**(9), 661–675 (2011). https://doi.org/10.1016/j.ijmecsci.2011.04.001
2. Abdelkhalek, S., Zahrouni, H., Potier-Ferry, M., Legrand, N., Montmitonnet, P., Buessler, P.: Coupled and uncoupled approaches for thin cold rolled strip buckling prediction. Int.J. Mater. Form. **2**(Suppl. 1), 833–836 (2009). https://doi.org/10.1007/s12289-009-0547-0
3. Cometa, A., et al.: Experimental investigation of pinching phenomena in cold rolling of thin steel sheets. In: AIP Conference Proceedings, vol. 2113 (2019). https://doi.org/10.1063/1.5112560
4. Cometa, A., Geijselaers, H.J.M., van den Boogaard, A.H., Wentink, D.J., Hol, C.W.J., Jacobs, L.J.M.: Experimental study on the mechanism of pinching in cold-rolling processes. Steel Res. Int. **93**(8) (2022). https://doi.org/10.1002/srin.202100812
5. Fischer, F., Rammerstorfer, F., Friedl, N.: Residual stress-induced center wave buckling of rolled strip metal. J. Appl. Mech. Trans. ASME **70**(1), 84–90 (2003). https://doi.org/10.1115/1.1532322
6. Linghu, K., et al.: 3D FEM analysis of strip shape during multi-pass rolling in a 6-high CVC cold rolling mill. Int. J. Adv. Manuf. Technol. **74**, 1733–1745 (2014). https://doi.org/10.1007/s00170-014-6069-z
7. Moazeni, B., Salimi, M.: Investigations on relations between shape defects and thickness profile variations in thin flat rolling. Int. J. Adv. Manuf. Technol. **77**(5–8), 1315–1331 (2015). https://doi.org/10.1007/s00170-014-6544-6
8. Nakhoul, R., Montmitonnet, P., Legrand, N.: Manifested flatness defect prediction in cold rolling of thin strips. Int. J. Mater. Form. **8**(2), 283–292 (2015). https://doi.org/10.1007/s12289-014-1166-y
9. Nakhoul, R., Montmitonnet, P., Potier-Ferry, M.: Multi-scale method for modeling thin sheet buckling under residual stresses in the context of strip rolling. Int. J. Solids Struct. **66**, 62–76 (2015). https://doi.org/10.1016/j.ijsolstr.2015.03.028
10. Roberts, W.L.: Cold Rolling of Steel. Marcel Dekker Inc., New York and Basel (1978)
11. Tieu, A., Zhu, H., Lu, C., You, C., Jiang, Z., D'Alessio, G.: Modelling of friction coefficient in cold strip rolling. Mater. Sci. Forum **505-507**(Part 2), 1285–1290 (2006). https://doi.org/10.4028/0-87849-990-3.1285
12. Wang, Q.L., Sun, J., Liu, Y.M., Wang, P.F., Zhang, D.H.: Analysis of symmetrical flatness actuator efficiencies for UCM cold rolling mill by 3D elastic-plastic FEM. Int. J. Adv. Manuf. Technol. **92**, 1371–1389 (2017). https://doi.org/10.1007/s00170-017-0204-6
13. Wang, X.C., Yang, Q., Jiang, Z.Y., Xu, J.W.: Research on the improvement effect of high tension on flatness deviation in cold strip rolling. Steel Res. Int. **85**, 1560–1570 (2014). https://doi.org/10.1002/srin.201400048
14. Yan, X., Sun, J., Xiong, S.: Effects of lubricants on the rolling performances of cold rolled copper strips. Procedia Eng. **207**, 2227–2232 (2017). https://doi.org/10.1016/j.proeng.2017.10.986